Acta Pharmacologica Sinica

www.nature.com/aps

ARTICLE

β-arrestin 2 is essential for fluoxetine-mediated promotion of hippocampal neurogenesis in a mouse model of depression

Chen-xin Li[2], Ying Zheng[2], Hong Zhu[1], Cheng-wu Li[2], Zhang He[2], Cong Wang[1], Jian-hua Ding[1], Gang Hu[1,2] and Ming Lu[1,3]

Over the last decade, the roles of β-arrestins in the treatment of neuropsychological diseases have become increasingly appreciated. Fluoxetine is the first selective serotonin reuptake inhibitor developed and is approved for the clinical treatment of depression. Emerging evidence suggests that fluoxetine can directly combine with the 5-HT receptor, which is a member of the G protein-coupled receptor (GPCR) family, in addition to suppressing the serotonin transporter. In this study, we prepared a chronic mild stress (CMS)-induced depression model with β-arrestin2$^{-/-}$ mice and cultured adult neural stem cells (ANSCs) to investigate the involvement of the 5-HT receptor-β-arrestin axis in the pathogenesis of depression and in the therapeutic effect of fluoxetine. We found that β-arrestin2 deletion abolished the fluoxetine-mediated improvement in depression-like behaviors and monoamine neurotransmitter levels, although β-arrestin2 knockout did not aggravate CMS-induced changes in mouse behaviors and neurotransmitters. Notably, the β-arrestin2$^{-/-}$ mice had a shortened dendritic length and reduced dendritic spine density, as well as decreased neural precursor cells, compared to the WT mice under both basal and CMS conditions. We further found that β-arrestin2 knockout decreased the number of proliferating cells in the hippocampal dentate gyrus and suppressed the proliferative capability of ANSCs in vitro. Moreover, β-arrestin2 knockout aggravated the impairment of cell proliferation induced by corticosterone and further blocked the fluoxetine-mediated promotion of mouse hippocampal neurogenesis. Mechanistically, we found that the 5-HT$_{2B}$R-β-arrestin2-PI3K/Akt axis is essential to maintain the modulation of hippocampal neurogenesis in depressed mice. Our study may provide a promising target for the development of new antidepressant drugs.

Keywords: β-arrestin2; 5-HT$_{2B}$R; fluoxetine; neural stem cell; neurogenesis; depression

Acta Pharmacologica Sinica (2021) 42:679–690; https://doi.org/10.1038/s41401-020-00576-2

INTRODUCTION

Depression is a prevalent and serious psychiatric disorder with high mortality and morbidity that is characterized by lack of pleasure, depressed mood, hopelessness, reduced motivation, and suicidal thoughts [1]. It is predicted that depression, known as the "first psychological killer", will be the leading public health problem and the most prevalent cause of disease burden globally by 2030 [2–5]. Over the past few decades, studies have shown that the volume and weight of the frontal cortex and hippocampus in depression patients were significantly reduced compared with those in healthy controls. Specifically, the decrease in the volume of neurons, the length and number of dendritic branches, and nerve regeneration were verified in depression patients [6, 7]. The causes of depression remain obscure thus far; however, multiple hypotheses have been proposed to clarify the pathogenesis of depression. Among these hypotheses, the monoaminergic hypothesis has received increased attention in neurobiological studies of depression and is the basis for various antidepressant drugs.

The classic prescribed drugs for the treatment of depression are selective serotonin reuptake inhibitors (SSRIs), such as fluoxetine (FLX). Fluoxetine acts on the serotonin transporter and improves patients' emotion by increasing the concentration of synaptic cleft 5-HT in depression-related brain regions such as the prefrontal cortex and hippocampus. Fluoxetine has also been shown to alleviate depression-like behavior and promote adult neurogenesis in the rodent hippocampus [8–11]. However, elevated 5-HT can cause sedation, drowsiness, and a range of behavioral responses, even affecting temperature regulation and motor function. Therefore, identifying more effective and potential molecular targets to develop novel antidepressants is urgently needed. Fortunately, a number of recent studies have explored new mechanisms of SSRI action. Emerging evidence suggests that diverse SSRIs, including fluoxetine, can bind to several 5-HT receptors and function as receptor agonizts [12]. The effect of SSRIs is inhibited in mice lacking the serotonin 5-HT$_{2B}$ receptor [13]. All these findings indicate that 5-HT receptors play an important role in the treatment of depression.

G-protein-coupled receptors (GPCRs), including the 5-HT$_{2B}$ receptor, are the largest family of membrane protein receptors and can be activated by multiple extracellular ligands. They can participate in the regulation of proliferation, differentiation,

[1]Jiangsu Key Laboratory of Neurodegeneration, Department of Pharmacology, Nanjing Medical University, Nanjing 211166, China; [2]Department of Pharmacology, Nanjing University of Chinese Medicine, Nanjing 210023, China and [3]Neuroprotective Drug Discovery Key Laboratory, Department of Pharmacology, Nanjing Medical University, Nanjing 211166, China
Correspondence: Gang Hu (ghu@njmu.edu.cn) or Ming Lu (lum@njmu.edu.cn)
These authors contributed equally: Chen-xin Li, Ying Zheng

Received: 31 August 2020 Accepted: 8 November 2020
Published online: 1 February 2021

chemotaxis, and communication in various physiological and pathological processes [14]. There are typically two types of signal transduction pathways in which GPCRs participate to trigger cellular responses: the classic G protein-dependent pathway and the β-arrestin (Arrb)-dependent pathway. GPCRs have been found to couple to β-arrestins, which are recruited to GPCRs and trigger receptor desensitization and internalization [15]. β-arrestins also activate other nonclassic pathways, such as PI3K/AKT and ERK1/2 signaling, to regulate cell proliferation and apoptosis, leading to multitudinous physiological responses [16–18]. Particularly, Arrb1 knockout mice showed reduced neural precursor proliferation in the subgranular zone (SGZ), which could be rescued by selective viral expression of Arrb1 [16]. In addition, a previous study reported that the effect of fluoxetine on motor behavior was hampered in Arrb2 knockout mice [8]. However, the involvement of β-arrestins in the antidepressant effect of fluoxetine and in depression-induced impairment of neurogenesis requires further exploration.

Therefore, the present study was designed to clarify the link between the GPCR-β-arrestin signaling pathway and fluoxetine-enhanced neurogenesis in a mouse model of depression. We used Arrb2 KO mice to prepare the chronic mild stress (CMS) model, administered fluoxetine to the mice and then detected depressive behavior and adult neurogenesis in the dentate gyrus. We found that Arrb2 is essential for the antidepressant effect of fluoxetine and the enhancement of neurogenesis in the CMS-induced mouse model. To investigate the mechanism underlying Arrb2-regulated neurogenesis in depression, we cultured Arrb2-deficient adult neural stem cells (ANSCs) to prepare a corticosterone-challenged model. The results showed that deletion of Arrb2 inhibited the proliferation of ANSCs and that fluoxetine promoted ANSC proliferation through the Arrb2-mediated 5-HT_{2B} receptor/PI3K/Akt pathway.

MATERIALS AND METHODS

The research protocol was approved by the Institutional Animal Care and Use Committee of Nanjing Medical University.

Animals

Two-month-old C57BL/6 (male, 18–22 g) mice were purchased from the Comparative Medicine Center of Nanjing University (Nanjing, China) (Animal Production License no. SCXR20100004). Mice with each genotype (Arrb2$^{+/+}$ and Arrb2$^{-/-}$) were randomly divided into the control, CMS and CMS + FLX groups. All animals were maintained under standard laboratory conditions (12/12 h light–dark cycle, constant humidity and temperature (25 °C) with free access to food and water) unless otherwise indicated.

Animal model and drug administration

The CMS model, a widely used depression model [19], was established as previously described [20]. The major procedures include ice water stimulation (10 min), clipping (10 min), pairing (2 h), cage tilt (45°, 12 h), restraints (12 h), wet cage (12 h), empty cage (12 h), food and water deprivation (12 h), continuous light (12 h), reversed light/dark cycle (24 h), etc. Two to three stimuli were given daily, and the same stimulus could not occur within three days; this schedule lasted for 8 weeks. The sucrose preference was tested every week during the CMS modeling. Between 8 and 12 weeks, fluoxetine (FLX) (10 mg/kg every day) was intraperitoneally injected daily. Furthermore, the mice were injected with bromodeoxyuridine (50 mg/kg, ip) daily on days 88–90.

Behavioral evaluations

Sucrose preference test. The sucrose preference test (SPT) was performed as described previously [21]. At 72 h before the test, all mice were habituated to 1% sucrose solution: 2 bottles of 1% sucrose solution (w/v) were placed in each cage. Then, 24 h later, the mice were deprived of water and food for 24 h followed by the SPT: each mouse was given 2 bottles that were placed on the cage containing 1% sucrose solution (w/v) and tap water to drink freely for 12 h. Six hours later, two bottles were exchanged to avoid location effects. Twelve hours later, the consumption of tap water and sucrose solution was recorded. The sucrose preference was calculated as sucrose preference (%) = (sucrose solution consumption)/(sucrose solution consumption + tap water consumption) × 100%.

Forced swimming test. A forced swimming test (FST) was carried out, and the total immobility was estimated as described in a previous report [22]. For the FST, mice were placed in a transparent glass beaker (14 cm diameter × 20 cm height containing 23–24 °C, 13 cm deep water) for 6 min. After the first 2 min of adaptation time, the behavior over the next 4 min was monitored. The 6 min test session was immobility scored and videotaped using automated TST/FST analysis software of Clever Systems.

Social approach-avoidance test. The social approach-avoidance test in mice was based on a previous report [23]. Mice were placed in a novel arena (40 × 27 × 20 cm). After 5 min of habituation, an empty cage (object stimulus; 12 × 8 × 8 cm) was placed on one side, and an identical cage containing an unknown male mouse (social stimulus) was placed on the other side wall of the arena for 10 min. Before each trial, the arena was cleaned with 75% alcohol. The contact behavior was defined as active sniffing, which was defined as the range of the nasal tip of the mice within 2 cm of the cage. The latency of the first exposure to the social cage and the preference index (=experimental mouse exposure to social cage time/exposure to empty cage time) were recorded.

Novelty-suppressed feeding test. For the novelty-suppressed feeding (NSF) test, the food pellets were removed from the mouse cages the day before testing. Twenty-four hours after food removal, the mice were transferred to a clean holding cage in the testing room. The testing apparatus consisted of a square open field (60 × 60 × 25 cm). A piece of chow was placed in the center of the testing apparatus. Each mouse was placed in the testing apparatus, and the time until the first feeding episode was recorded for up to 10 min [24, 25].

High-performance liquid chromatography analysis

NE, 5-HT and DA in the hippocampus were measured by high-performance liquid chromatography with an electrochemical detector (Ultimate 3000 Auto sampler) as described previously [26]. Hippocampal tissues were homogenized in extract solution, which consisted of 0.1 M $HClO_4$ and 0.1 mM EDTA buffer, and the mixtures were centrifuged at a speed of 20,000 r/min for 30 min at 4 °C. Then, 50 μL of the resultant supernatant was injected into the liquid chromatography system equipped with a reversed-phase C18 column (2.2 μm, 120 Å, 2.1 × 100 mm, Dionex) and was detected by an ESA Coulochem III Electrochemical Detector. The detector was set at 350 mV. The mobile phase consisted of 90 mM NaH_2PO_4, 1.7 mM *1*-octanesulfonic acid, 50 mM citrate, 50 μM EDTA-$_2$Na, and acetonitrile (0.05 w/v) (pH 2.6). The identification and purity were evaluated by chromatographic peaks. Quantitative evaluations were performed by comparing the retention times and peak areas with those of standard solutions.

Immunohistochemistry

The hippocampal slices were selected according to the mouse brain map. For β-arrestin2/NeuN colocalization and MAP-2 immunofluorescence, midbrain sections were treated for DNA denaturation but without H_2O_2 disposition. At the end of incubation in phosphate buffered saline (PBS)/0.1% Triton X-100/5% bovine serum albumin (BSA) for 1 h, the sections were

incubated with polyclonal antibodies, including mouse anti-NeuN (1:100, Millipore), rabbit anti-β-arrestin2 (1:500, Abcam), mouse anti-BrdU (1:5000, Millipore), rabbit anti-DCX (1:500, Abcam), rabbit anti-Ki67 (1:1000, Cell Signaling), and mouse anti-nestin (1:100, Millipore), and at 4 °C overnight, followed by secondary antibody for 1 h at room temperature (22 ± 2 °C). Fluorescent mounting media was applied before placing coverslips, and wet mounted sections were dried in the dark. For visualization and photography, specimens were observed with Microbrightfield Stereo Investigator software (Williston, VT, USA).

Golgi staining

Mice were deeply anesthetized, and brains were quickly removed and used to prepare for Golgi impregnation using the FD Rapid Golgi Stain Kit (FD Neurotechnologies; Baltimore, MD). Briefly, the brains were incubated in a mixture of solutions A and B for 14 days at room temperature in the dark and received solution C for 3–7 days at room temperature. Then, the brains were embedded in OCT and rapidly frozen in liquid nitrogen. Tissue was cut into 100 μm slices with a cryostat at −20 to −22 °C and stained with a mixture of solutions D and E for 10 min. Slides were then dehydrated, cleaned in xylene and coverslipped with neutral balsam. Images were captured on an Olympus BX51 microscope (100× magnification). Spines from granular neurons were counted and normalized against the total dendrites.

NSC culture and neurosphere assay

Primary cultures of ANSCs and neurosphere assays were established in our previous publication [27]. Briefly, the brains of 2-month-old male C57BL/6J mice were microdissected to obtain the subventricular zone and hippocampus. Tissues were cut into small pieces of 1–2 mm^3 using a 5 mL disposable syringe to blow and beat slowly. After centrifugation, cells were carefully dissociated by passaging in fire-polished Pasteur pipettes and resuspended in serum-free medium consisting of Dulbecco's modified Eagle's medium/F12 (1:1) medium (Gibco) supplemented with 2% B27 (Gibco), 20 ng/mL EGF, and 20 ng/mL bFGF (Peprotech).

Cell proliferation assays

Cell proliferation and cell differentiation assays were described in our previous publication [28]. Briefly, neurospheres were collected and gently mechanically dissociated. Dissociated cells were plated on 24-well culture plates coated with poly-*L*-ornithine (10 μg/mL) and laminin (5 μg/mL) and cultured for 48 h. The cells were incubated for exactly 60 min with 10 μM BrdU and then fixed and washed. DNA was denatured by treating the cells for 30 min with 2 N HCl at 37 °C. The cells were extensively washed and blocked with 5% BSA (40 min). The primary mouse anti-BrdU antibody (1:1000, Millipore) was applied and incubated for 1 h at 37 °C followed by goat anti-mouse FITC antibody (1:1000, Invitrogen). The cells were mounted with antifade medium (Dako Cytomation) and DAPI.

Western blotting

Total cellular proteins of neurospheres were extracted with homogenization buffer. Equivalent amounts of extracted proteins (50 μg) were resolved by SDS-PAGE and electroblotted onto PVDF membranes (Amersham Biosciences). After the background staining was blocked with 5% skim milk in PBS, the membranes were incubated in primary antibodies including rabbit anti-β-arrestin2 (1:500, Santa Cruz), rabbit anti-pPI3K (1:1000, Cell Signaling), rabbit anti-PI3K (1:1000, Cell Signaling), rabbit anti-pAKT (1:500, Cell Signaling), rabbit anti-AKT (1:500, Cell Signaling), rabbit anti-pErk (1:500, Cell Signaling), rabbit anti-Erk (1:500, Cell Signaling), rabbit anti-pGSK3β (1:500, Cell Signaling), and rabbit anti-GSK3β (1:500, Cell Signaling) overnight at 4 °C. Immunoreactive proteins were detected using HRP-conjugated secondary antibodies and an ECL kit (Amersham Biosciences) according to the manufacturer's instructions. The membranes were scanned and analyzed in an Omega 16ic Chemiluminescence Imaging System (Ultra-Lum, Claremont, CA, USA).

Quantitative real-time PCR

Total RNA from dissected tissues was extracted using TRIzol Reagent (Life Technologies). One microgram of total RNA was used for cDNA synthesis using the PrimeScript RT Reagent Kit (TaKaRa). cDNA was stored at −80 °C until use. Real-time PCR was performed using the Applied Biosystems StepOne Real-Time PCR System with SYBR Green PCR Master Mix (Applied Biosystems) according to the manufacturer's protocol. The PCR conditions were 15 min at 95 °C, followed by 45 cycles of 15 s at 95 °C and 30 s at 60 °C. The following primers were used (5′ to 3′): GAPDH, CCAGC TACTC GCGGC TTTA (forward) and GTTCA CACCG ACCTT CACCA (reverse); 5-HT_{1A}R, TAGCT GTCTG AGCGA CACAC (forward) and TCCAG AAACC CCATC CTCCC (reverse); 5-HT_{1B}R, AAGCA AGGCT CTCTC TTCTGG (forward) and AGGGA TACCC ATCCA TCACCA (reverse); 5-HT_{2A}R, TCTTT AAGGC GGGGA GTTGCT (forward) and TTTTG CTCAT TGCTG ATGGA CTG (reverse); 5-HT_{2B}R, CTCGG GGGTG AATCC TCTGA (forward) and CCTGC TCATC ACCCT CTCTCA (reverse); 5-HT_{2C}R, TGCAT TCATT CCTTG TGCAC (forward) and ATATC TAGGT AGTGG CCAGA (reverse).

Statistical analysis

The data are expressed as the mean ± SEM. Mean value differences were assessed using two-way or one-way ANOVA followed by the post hoc LSD test. Significant differences existed at $P < 0.05$.

RESULTS

Arrb2 is necessary for the fluoxetine-mediated improvement in the mouse physiological state and depression-like behaviors in the CMS model

To investigate the involvement of β-arrestins in the pathogenesis of depression and in the therapeutic effect of fluoxetine, we prepared a CMS-induced mouse model according to the protocol shown in Fig. 1a. First, to observe whether there was a change in the expression of β-arrestins in the hippocampus of the depressive mice, we detected the protein levels of β-arrestins by Western blotting. The expression of Arrb2 in the CMS-induced mice was significantly lower than that in the control mice, but there was no difference in the expression of Arrb1 (Fig. S1a, b). Moreover, we colabeled NeuN and β-arrestin1/2 in the hippocampus by immunofluorescence. Consistently, we found that the number of $NeuN^+/Arrb2^+$ double-positive cells in the mouse model of CMS was reduced compared with that in the control group, but there was no significant difference in the number of $NeuN^+/Arrb1^+$ cells between the control and CMS groups (Fig. S1c, d).

Given the decreased expression of β-arrestin2 in the hippocampus of the CMS-treated mice, we further prepared a CMS model and treated the WT and $Arrb2^{-/-}$ mice with fluoxetine. As shown in Fig. 1b, the survival rate of the $Arrb2^{+/+}$ mice was 75% at the end of the 12-week CMS modeling, while the survival rate of the $Arrb2^{-/-}$ mice was only 62%. There were also differences in the physiological state of the mice during CMS. We found that the physiological status scales of the CMS-treated mice were decreased, especially in the $Arrb2^{-/-}$ mice. Fluoxetine-mediated improvement of the physiological status was observed in the $Arrb2^{+/+}$ mice but was blocked in the $Arrb2^{-/-}$ mice in response to CMS (Fig. 1c). However, in terms of weight gain, the body weight of the CMS-induced mice was lost during CMS modeling, there was no difference between the $Arrb2^{+/+}$ and $Arrb2^{-/-}$ mice, and fluoxetine failed to increase the body weight in both types of mice (Fig. 1d).

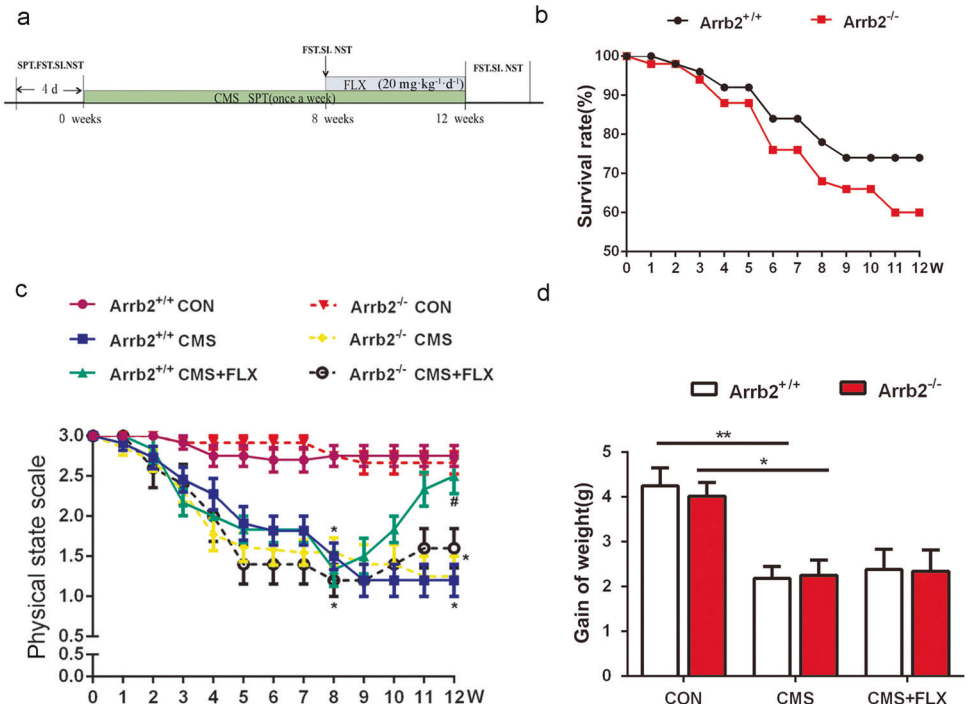

Fig. 1 The effect of Arrb2 on the general state of mice with CMS. a The protocol of the CMS model and fluoxetine treatment. **b** Survival rate, (**c**) physical state score, and (**d**) weight gain in the mice with both genotypes with or without fluoxetine treatment. $n = 10–13$ per group. All data are presented as the mean ± SEM. $^{*}P < 0.05$; $^{**}P < 0.01$ vs. the indicated group.

For depressive-like behaviors, we performed sucrose preference tests, FSTs, NSF tests, and social approach-avoidance (SI) tests. Fluoxetine improved all depressive parameters in the wild-type mice, as evidenced by an increase in the sucrose preference percentage over the 12-week model (Fig. 2a, b). Fluoxetine also decreased the immobility time in the FST (Fig. 2c), reduced the latency to feeding and sniffing in the NSF and SI tests, and increased the preference index in the SI test in the WT mice (Fig. 2d–f). Interestingly, Arrb2 knockout did not aggravate depression-like behaviors during CMS but could eliminate the fluoxetine-mediated improvement of depression-like behaviors in the CMS model.

Fluoxetine regulation of the abnormalities of neurotransmitters and corticosterone is dependent on the presence of Arrb2

The abnormal secretion of neurotransmitters is the main feature of depression. We detected the contents of 5-HT, DA and NE in the hippocampus of mice by high-performance liquid chromatography. The results showed that the levels of 5-HT and its metabolite 5-HIAA (Fig. 3a, b), as well as DA (Fig. 3c), were significantly decreased in both the $Arrb2^{+/+}$ and $Arrb2^{-/-}$ mice in the CMS model compared with those in the control groups. Fluoxetine treatment could almost raise the concentrations of these neurotransmitters to the normal levels in the WT mice but not in the $Arrb2^{-/-}$ mice. However, the contents of NE and DA metabolites, including DOPAC and HVA, were not significantly different among the three groups of WT mice (Fig. 3d–f). Notably, the level of NE in the CMS group was noticeably decreased compared with that in the CON group of $Arrb2^{-/-}$ mice, but fluoxetine failed to reverse this decrease (Fig. 3f). These results suggest that β-arrestin2 is involved in the fluoxetine-mediated regulation of partial neurotransmitters in the CMS model.

During the development of depression, pathological characteristics of HPA axons are observed, and the main change is the elevation of corticosterone (CORT) content in cerebrospinal fluid and serum. Therefore, the corticosterone content in mouse serum was detected by a corticosterone kit (Corticosterone ELISA Kit, Cayman, No. 501320). The results showed that the CMS model had a significant increase in serum corticosterone in the mice with both genotypes compared with that in the corresponding control group, indicating that there was hyperactivity of the HPA axis of the CMS-induced mice. However, there was no significant difference in the corticosterone content between the two genotypes. After fluoxetine treatment, the corticosterone content in the $Arrb2^{+/+}$ mice was decreased significantly, but fluoxetine failed to reduce the corticosterone levels in the CMS-treated $Arrb2^{-/-}$ mice, which were significantly higher than those in the $Arrb2^{+/+}$ treatment group (Fig. S2). This result suggests that β-arrestin2 knockout interferes with the regulatory effect of fluoxetine on the HPA axis in the CMS model.

The presence of Arrb2 is crucial for the neurotrophic effects of fluoxetine in the hippocampus of the CMS-induced mice

To identify the role of β-arrestin2 in the pathogenesis of depression and the antidepressant effect of fluoxetine, we examined neuronal development and survival by labeling DCX^{+} and $MAP\text{-}2^{+}$ cells in the hippocampus. We found that the $Arrb2^{-/-}$ mice showed a reduced number of DCX-positive cells compared with the WT mice. Furthermore, the effect of fluoxetine on neuronal development was significantly weaker in the $Arrb2^{-/-}$ mice than in the WT mice (Fig. 4a, b). Moreover, immunostaining of MAP-2 demonstrated that compared with the WT mice, the $Arrb2^{-/-}$ mice showed reduced MAP-2 expression after CMS. Fluoxetine significantly restored the expression of MAP-2 protein in the WT mice but not in the $Arrb2^{-/-}$ mice (Fig. 4c).

To further study the role of Arrb2 in the neurotrophic effect of fluoxetine, we used Golgi staining to determine the numbers of dendritic spines and the length of dendritic branches in the mouse hippocampus. As shown in Fig. 4d–f, the neuronal dendritic length in the $Arrb2^{-/-}$ mice was lower than that in the $Arrb2^{+/+}$ mice in the basal state. The dendritic length and dendritic spine density in both types of mice decreased significantly in the CMS group, and neuronal damage was

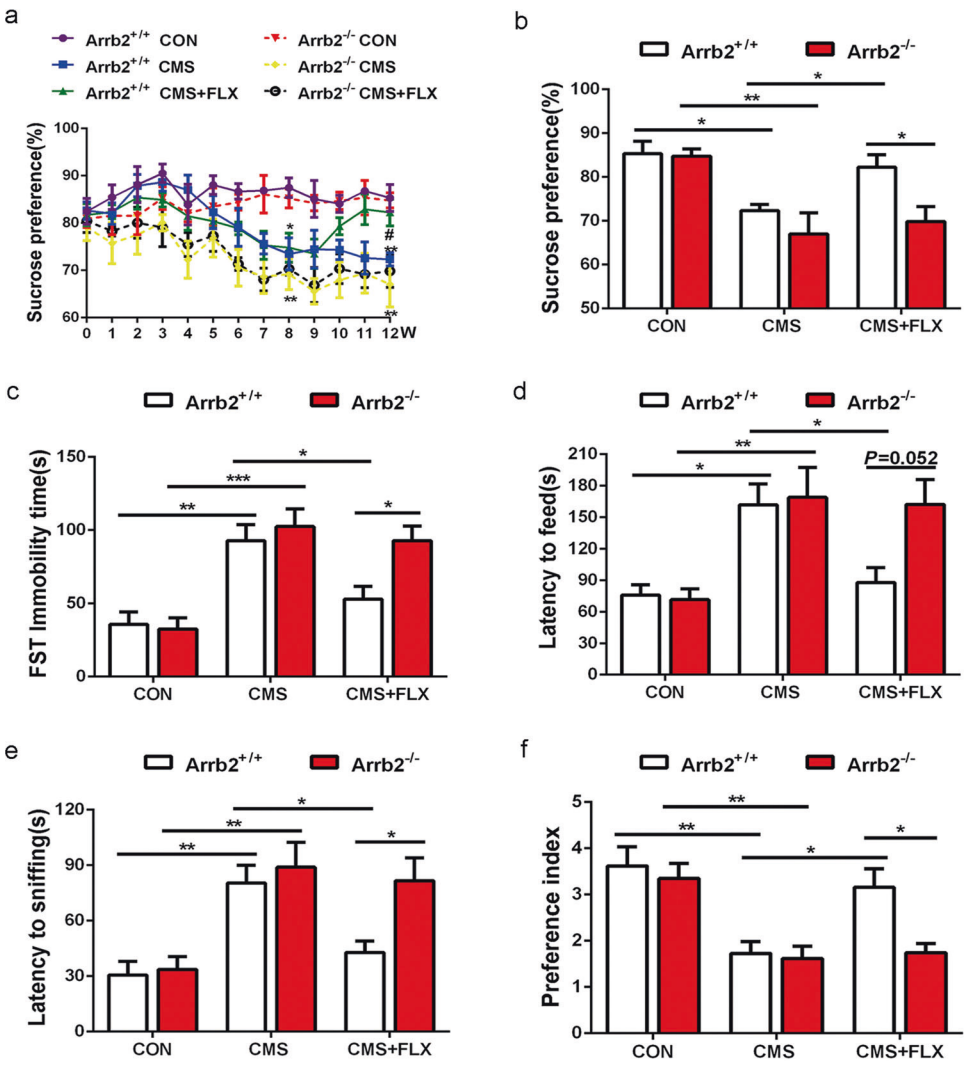

Fig. 2 The effect of Arrb2 on depression-like behavior in the fluoxetine-treated CMS-induced mice. a Changes in the sucrose preference percentage of the mice over 12 weeks. **b** Sucrose preference percentage of the mice in the last week. **c** The immobility times in the forced swimming test (FST) and (**d**) the latency to feeding in the novelty-suppressed feeding test (NSF). **e**, **f** The latency to sniffing and the preference index in the social approach-avoidance test (SI). $n = 8–12$ per group. All data are presented as the mean ± SEM. $^{*}P < 0.05$; $^{**}P < 0.01$ vs. the indicated group.

aggravated in the Arrb2$^{-/-}$ mice. After treatment with fluoxetine, the length of dendrites and the density of dendritic spines increased compared with those in the CMS group of WT mice. However, fluoxetine failed to improve the neuronal damage induced by CMS in the Arrb2$^{-/-}$ mice. These results indicate that the presence of β-arrestin2 is required for the neurotrophic effect of fluoxetine in the hippocampus of mice with CMS.

β-arrestin2 knockout inhibited cell proliferation in the hippocampus and abolished the effect of fluoxetine on neurogenesis in the CMS-induced mice

Next, we injected BrdU (50 mg/kg every day, ip, 3 d) to mark the proliferating cells in the mouse dentate gyrus. As shown in Fig. 5a, b, the Arrb2$^{-/-}$ mice showed reduced BrdU^{+} cells in the DG under basal conditions. β-arrestin2 knockout aggravated the decrease in the number of BrdU^{+} cells induced by CMS. Furthermore, fluoxetine increased BrdU^{+} cells in the WT mice but failed to attenuate the inhibition of cell proliferation in the DG of the Arrb2$^{-/-}$ mice. Ki67 can also mark cells in the proliferative period, and proliferating cell nuclear antigen (PCNA) is widely expressed in the late G1 and S periods and can be used as an index to evaluate the proliferative status of cells. Similarly, the Arrb2$^{-/-}$ mice showed fewer Ki67^{+} cells (Fig. 5c, d) and lower expression of PCNA (Fig. 5e, f) in both the control and CMS groups than the WT group. Fluoxetine treatment increased Ki67^{+} cells and PCNA expression in the WT mice, but β-arrestin2 deletion abolished the effect of fluoxetine on neurogenesis in the SGZ. These results suggest that β-arrestin2 plays a critical role in promoting hippocampal neurogenesis in the CMS-induced mouse model.

Arrb2 deficiency blocked the fluoxetine-mediated enhancement of proliferation of ANSCs in vitro

We selected brain tissue in the SGZ region from 2-month-old male mice, cultured neurospheres, and identified ANSCs by nestin and BrdU staining. The results showed that cultured neurospheres were BrdU^{+} ANSCs with proliferative activity, and ANSCs expressed the neural cell-specific marker Nestin (Fig. S3), indicating the stem cell activity of cultured ANSCs in vitro.

The F2 ANSCs were inoculated at a density of 1×10^5 cells/well into an untreated 24-well plate, and the diameter and number of neurospheres were observed 7 days later. The results showed that both the number and diameter of neurospheres in the

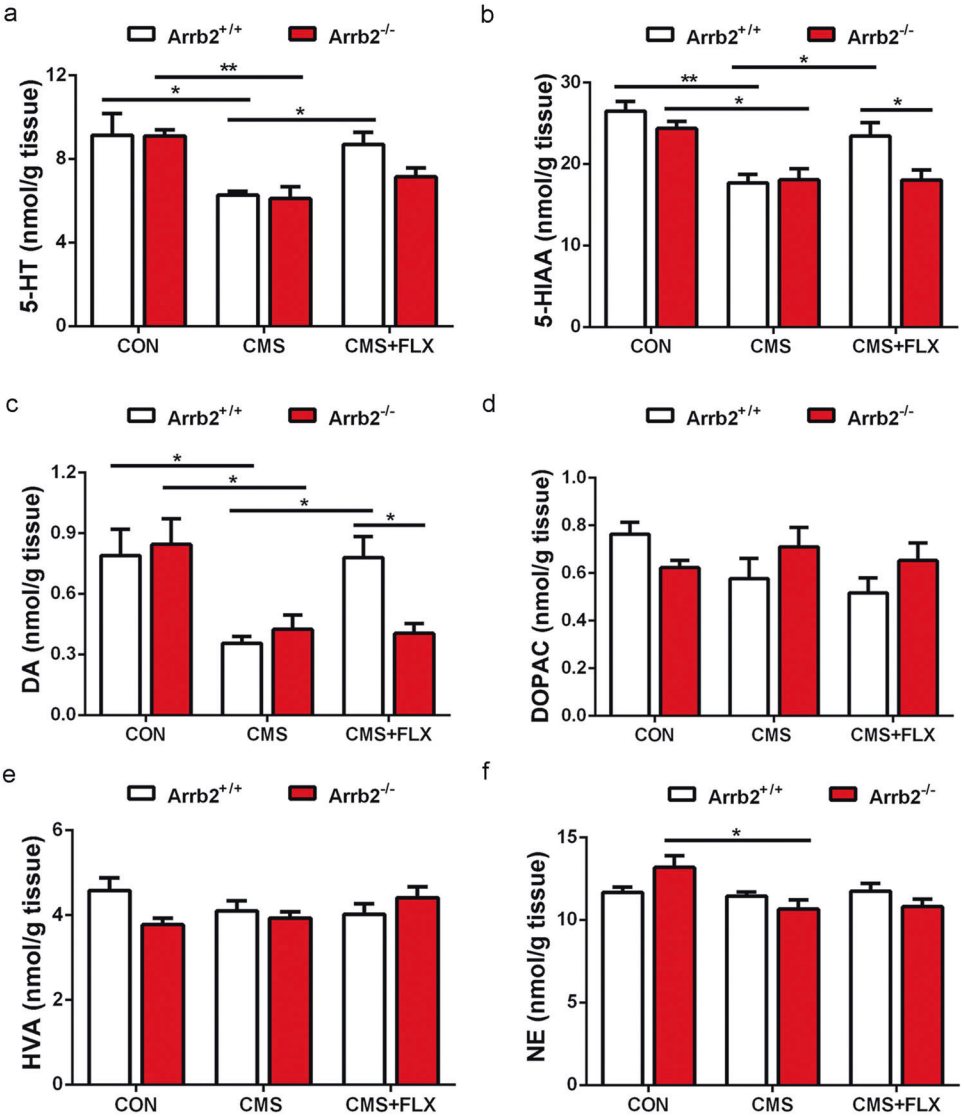

Fig. 3 The effect of Arrb2 on neurotransmitters and metabolites in the fluoxetine-treated CMS-induced mice. The levels of (**a**) 5-HT, (**c**) DA, (**f**) NE, and their metabolites (**b**) 5-HIAA, (**d**) DOPAC, and (**e**) HVA in the mouse hippocampus were analyzed by high-performance liquid chromatography. $n = 8–12$ per group. All data are presented as the mean ± SEM. $^{*}P < 0.05$; $^{**}P < 0.01$ vs. the indicated group.

$Arrb2^{-/-}$-derived ANSCs were lower than those in the ANSCs isolated from the $Arrb2^{+/+}$ mice, with a significant difference under basal conditions (Fig. 6a, b). This result suggests that β-arrestin2 knockout inhibited the self-renewal ability of ANSCs.

During the development of depression, elevation of corticosteroid content in plasma is a distinctive feature that may be involved in hippocampal atrophy. In vivo and in vitro experiments have shown that corticosteroids can significantly inhibit the proliferation of neural stem cells. Therefore, based on previous experiments [29], this study used 1 mM corticosteroid to simulate neural injury in vitro, followed by treatment with fluoxetine at 0.1, 1, and 10 μM for 72 h. As shown in Fig. 6c, we found that corticosteroids significantly inhibited the cell viability of both genotypes through CCK8 assays to detect the proliferative capacity of ANSCs. Furthermore, fluoxetine at 1 μM reversed the suppression of cell viability in the $Arrb2^{+/+}$ ANSCs but had no effect on the ANSCs isolated from the $Arrb2^{-/-}$ mice.

Next, BrdU analysis and Ki67 staining were carried out to evaluate the effect of β-arrestin2 on the proliferative capacity of ANSCs. Consistently, β-arrestin2 knockout aggravated the inhibition of ANSC proliferation in response to corticosterone challenge. Fluoxetine increased the number of $BrdU^{+}$ cells (Fig. 6d, e) and $Ki67^{+}$ cells (Fig. 6f, g) in the $Arrb2^{+/+}$ ANSCs but failed to rescue the decrease in proliferative cells induced by corticosterone in the $Arrb2^{-/-}$ ANSCs. The above results indicated that β-arrestin2 knockout significantly inhibited the proliferation of ANSCs and abolished the effect of fluoxetine in promoting cell proliferation in a corticosterone-stimulated mouse ANSC model.

Fluoxetine-enhanced ANSC proliferation via the β-arrestin2/PI3K/Akt signaling pathway

The PI3K/Akt pathway is involved in maintaining cell proliferation, survival and differentiation and plays a role in regulating nerve regeneration. In the present study, the effects of β-arrestin2 knockout on the signaling pathway related to cell proliferation were observed by detecting the expression of PI3K, Akt, and GSK3β. As shown in Fig. 7a–d, the levels of phosphorylated PI3K and phosphorylated Akt in the $Arrb2^{-/-}$ ANSCs were significantly lower than those in the $Arrb2^{+/+}$ groups. However, there was no change in the protein expression of p-GSK3β and total GSK3β

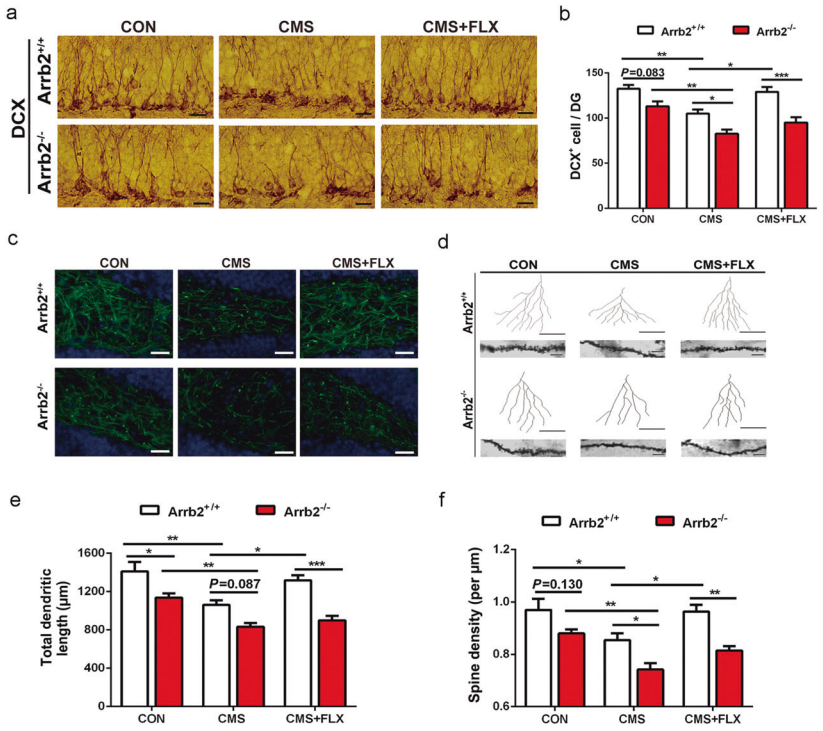

Fig. 4 The effect of Arrb2 on neuronal morphology and dendritic spine density in the fluoxetine-treated CMS-induced mice. **a** Immunohistochemistry of DCX and (**b**) quantitative analysis of positive cells in the hippocampal dentate gyrus (DG). **c** Immunofluorescence of MAP-2 in the hippocampal DG, scale bar: 50 μm. **d** Neuronal morphology is reflected in a two-dimensional map, scale bar: 100 μm. The dendritic spine was photographed under a 100× microscope, scale bar: 10 μm. **e**, **f** Quantitative analysis of total dendritic length and spine density is shown. $n = 4–6$ per group. All data are presented as the mean ± SEM. $^{*}P < 0.05$; $^{**}P < 0.01$; $^{***}P < 0.001$ vs. the indicated group.

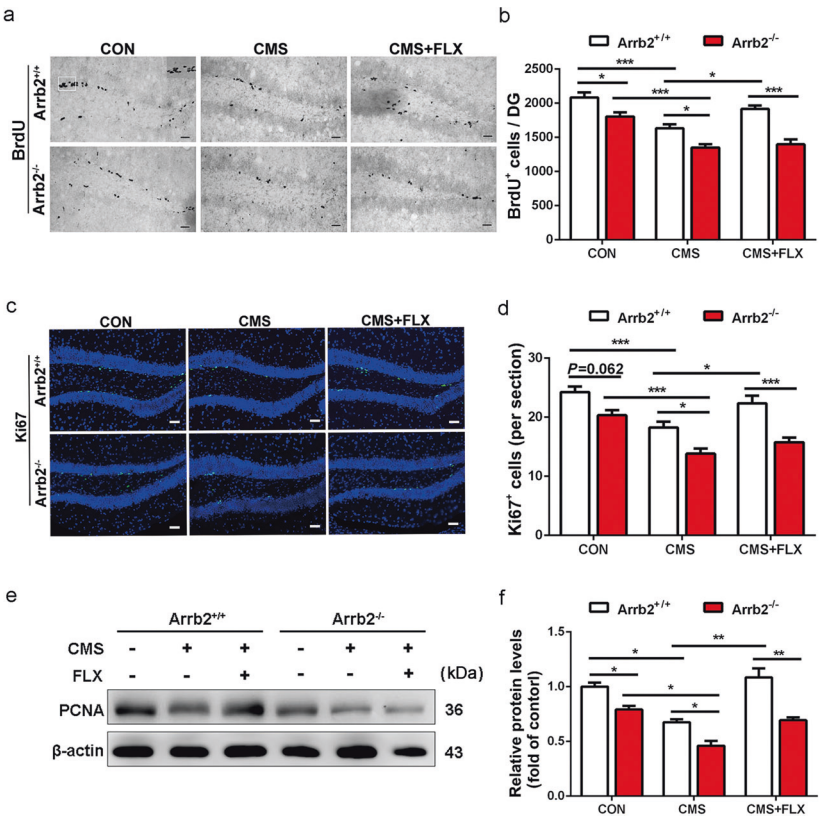

Fig. 5 The effect of Arrb2 on hippocampal neurogenesis in the fluoxetine-treated CMS-induced mice. **a**, **b** Immunohistochemistry of BrdU and quantitative analysis of positive cells in the hippocampal dentate gyrus (DG), scale bar: 50 μm. **c**, **d** Immunofluorescence of Ki67 and quantitative analysis of positive cells in the hippocampal DG, scale bar: 50 μm. **e**, **f** Western blotting for PCNA expression and quantitative analysis of PCNA protein levels in the hippocampus of mice. $n = 4–6$ per group. All data are presented as the mean ± SEM. $^{*}P < 0.05$; $^{**}P < 0.01$; $^{***}P < 0.001$ vs. the indicated group.

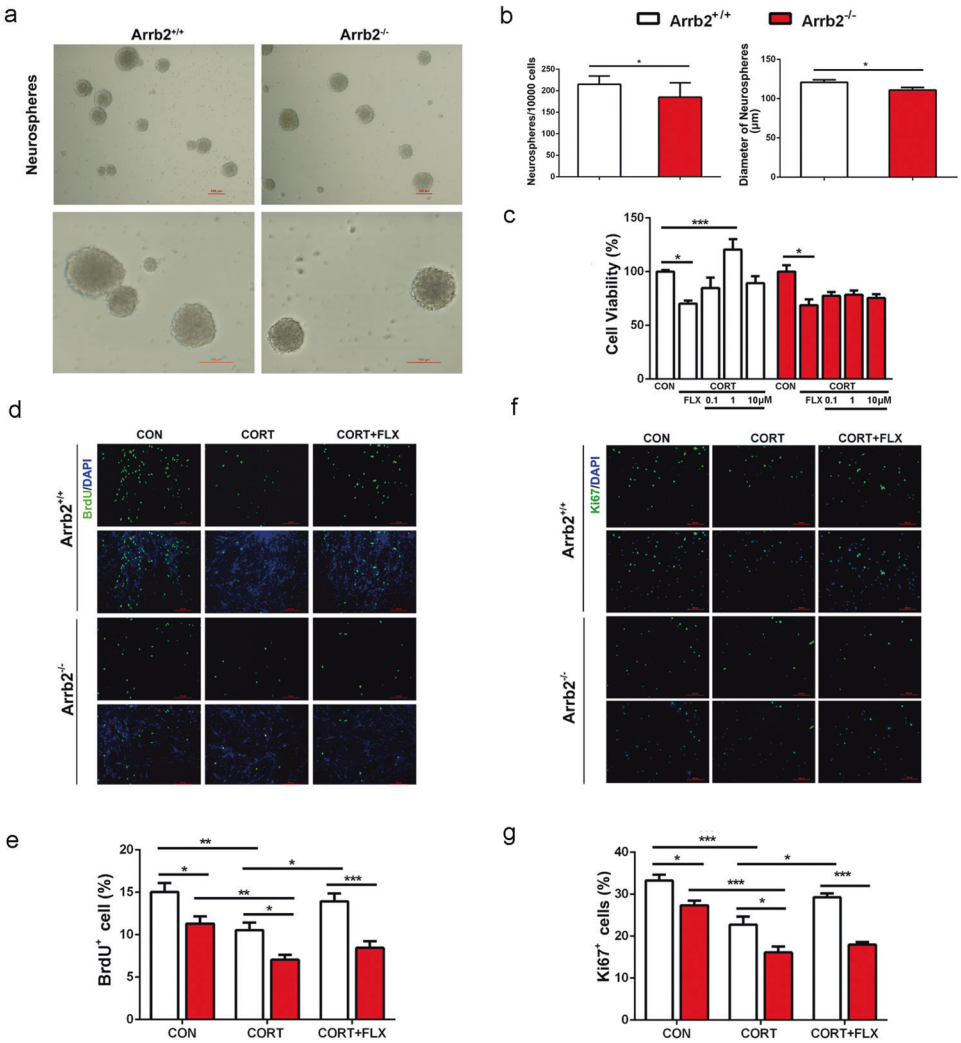

Fig. 6 The effect of Arrb2 on the self-renewal of neurospheres and the proliferation of adult neural stem cells in the CORT-induced model. a Brightfield image of SGZ neurosphere culture in vitro, scale bar: 100 μm. **b** Quantification of the number and diameter of cultured neurospheres. **c** Cell viability of ANSCs was detected by CCK8 assays. **d**, **e** Immunofluorescence of BrdU and quantitative analysis of positive cells in ANSCs. **f**, **g** Immunofluorescence of Ki67 and quantitative analysis of positive cells in ANSCs. scale bar: 100 μm. All data are presented as the mean ± SEM of four independent experiments. $^{*}P < 0.05$; $^{**}P < 0.01$; $^{***}P < 0.001$ vs. the indicated group.

between the two genotypes. After CORT incubation, the expression of p-PI3K and p-Akt in both genotypes decreased significantly, and fluoxetine treatment raised the levels of p-PI3K and p-Akt in the Arrb2$^{+/+}$-derived ANSCs alone. In contrast, the Arrb2$^{-/-}$ ANSCs showed resistance to the fluoxetine-mediated phosphorylation of the PI3K/Akt protein, suggesting that this pathway may be involved in the β-arrestin2-mediated proliferation of ANSCs.

To verify the above results, we used the PI3K pathway inhibitor LY294002 to observe its effect on fluoxetine-evoked proliferation in the Arrb2$^{+/+}$ ANSCs. LY294002 (5 μM, pretreatment for 1 h) abolished the increase in the number of BrdU^{+} cells induced by fluoxetine, although LY294002 itself had no effect on ANSC proliferation (Fig. 7e, f). These results suggest that β-arrestin2 knockout inhibits neural stem cell PI3K/Akt phosphorylation and the enhancement by fluoxetine. ANSC proliferation partially depends on activating the β-arrestin2-PI3K/Akt pathway.

The 5-HT$_{2B}$ receptor is required for the effect of fluoxetine in activating the β-arrestin2-PI3K/Akt pathway and promoting ANSC proliferation

β-arrestins need to be recruited to GPCRs, which in turn trigger downstream signal transduction. Previous studies have reported that fluoxetine can act directly on the 5-HT receptor, which is a member of the GPCR family, to play its role in regulating neurotransmission [12, 13]. In this study, the mRNA levels of different 5-HT receptor subtypes in ANSCs were detected by qPCR. The 5-HT$_{2B}$R expression was the highest among the subtypes in cultured ANSCs (Fig. 8a, b). In addition, some studies have shown that fluoxetine can bind to 5-HT$_{2B}$R and subsequently activate this receptor in serotonergic neurons. We thus speculated that 5-HT$_{2B}$R may be involved in the effect of fluoxetine on β-arrestin2-mediated proliferation in ANSCs. Therefore, the 5-HT$_{2B}$R inhibitor RS-127445 was used to observe the effects of fluoxetine in activating the PI3K/Akt pathway and in promoting cell proliferation. As shown in Fig. 8c, d, RS-127445 alone had no effect on the PI3K/Akt pathway and could not impact the proliferation of ANSCs. Interestingly, the fluoxetine-mediated activation of the PI3K/Akt pathway in the CORT model was eliminated by RS-127445. Consistent with this finding, the 5-HT$_{2B}$R inhibitor also abolished the effect of fluoxetine in promoting proliferation in the CORT-stimulated ANSCs (Fig. 8e, f). Collectively, these results indicate that 5-HT$_{2B}$R is required for the effect of fluoxetine on β-arrestin2-mediated proliferation in ANSCs.

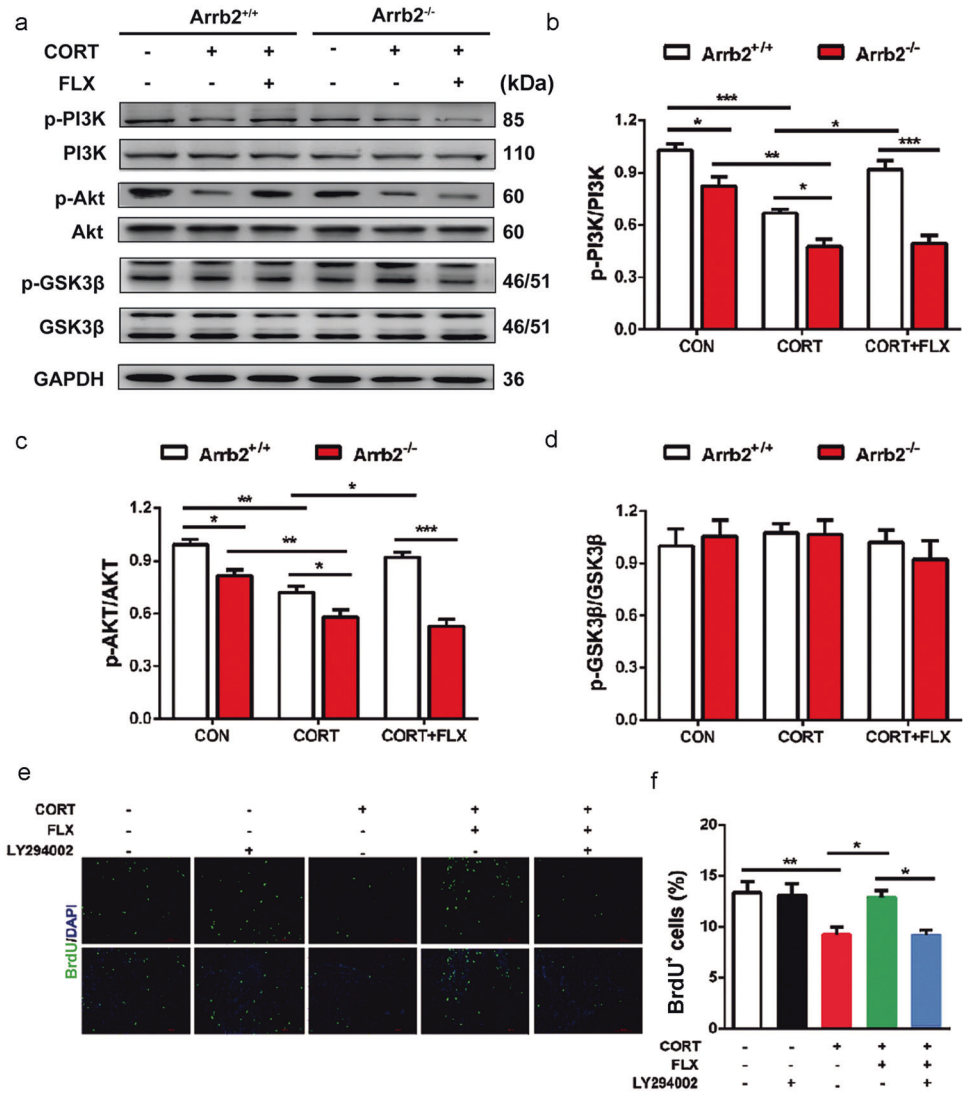

Fig. 7 The effect of Arrb2 on the PI3K/Akt signaling pathway in the CORT-challenged ANSC model. a Representative gel showing the WB results of PI3K/Akt/GSK3β expression in ANSCs. **b**–**d** Quantitative analysis of phosphorylated PI3K/Akt/GSK3β expression levels in ANSCs. **e** Immunofluorescence of BrdU in ANSCs and (**f**) quantitative analysis of positive cells in culture, scale bar: 100 μm. All data are presented as the mean ± SEM of four independent experiments. $^{*}P < 0.05$; $^{**}P < 0.01$; $^{***}P < 0.001$ vs. the indicated group.

DISCUSSION

At present, more than 120 million people live under the shadow of depression, and patients suffering from major depressive disorder are prone to suicide. Approximately 850,000 suicides occur every year, but few rapid, robust, and sustained antidepressants can be used clinically. Over the past decades, the monoaminergic neurotransmitter hypothesis has been regarded as the basis for the pathogenesis and therapeutics of depression. Fluoxetine is the first developed SSRI, which is approved for the clinical treatment of depression, bulimia nervosa, and obsessive-compulsive disorder. Fluoxetine improves patients' emotions by increasing the concentration of synaptic cleft 5-HT by suppressing the serotonin transporter. In recent years, fluoxetine has been shown to have multiple effects such as antioxidative, anti-inflammatory, antitumor, and neuroprotective effects in addition to the effects described by the serotonin hypothesis [11, 30–33]. Notably, emerging evidence suggests that fluoxetine can directly combine with the 5-HT receptor and subsequently activate signal transduction downstream of the receptor. It remains unknown whether the 5-HT receptor-mediated signaling pathway participates in fluoxetine-induced neuroprotection and neurogenesis.

The 5-HT receptor is a member of the GPCR family, which is the largest family of membrane protein receptors and has the largest number of drug targets. β-arrestins are a class of scaffolding proteins that can be recruited to GPCRs and negatively regulate G protein signaling. β-arrestins trigger receptor desensitization and internalization, as well as activation of the G protein-independent signaling pathway. β-arrestins can regulate cell proliferation and apoptosis and are involved in multitudinous physiological responses [34–36]. Over the last decade, the roles of 5-HTR-β-arrestin2 expressed in neurons have been associated with several physiological functions and neuropsychiatric disorders. For example, the 5-HT_{2A}R–β-arrestin interaction may be particularly important in receptor function in response to endogenous serotonin levels, which could have major implications in drug development for treating neuropsychiatric disorders such as schizophrenia. However, the involvement of the 5-HT receptor-β-arrestin axis in the pathogenesis of depression and in the therapeutic effect of fluoxetine are unclarified. Therefore, we detected the expression of β-arrestin1 and β-arrestin2 in the hippocampus of CMS-induced mice. We found that β-arrestin2, rather than β-arrestin1, was significantly decreased in depressive mice. Next, we focused on β-arrestin2 and further prepared a CMS

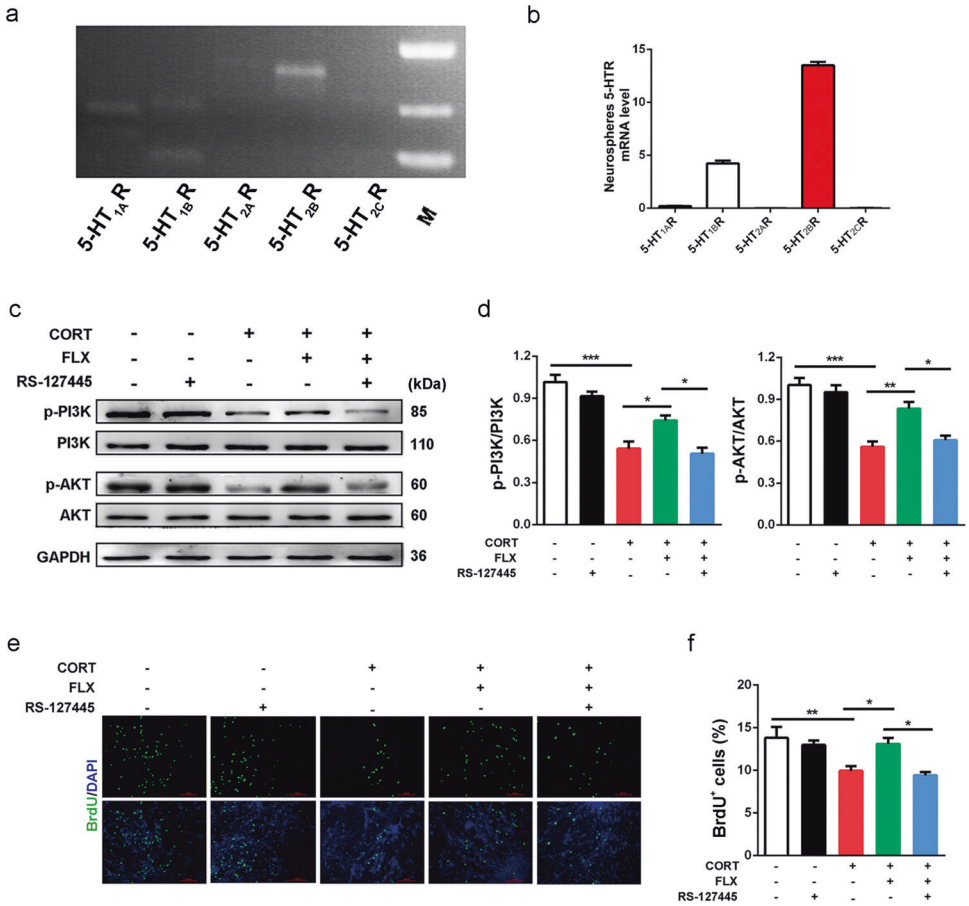

Fig. 8 The involvement of the 5-HT$_{2B}$R-β-arrestin2 axis in the fluoxetine-enhanced proliferation of the CORT-injured ANSCs. **a** Representative gel for PCR results of 5-HTR expressed on ANSCs. **b** Quantitative analysis of the 5-HTR mRNA levels in ANSCs. **c** Representative gel for the WB results of PI3K/Akt expression in ANSCs. **d** Quantitative analysis of phosphorylated PI3K/Akt expression. **e** Image of immunofluorescence staining for BrdU$^+$ cells in ANSCs. scale bar: 100 μm. **f** Stereology quantitative counting of BrdU$^+$ cells in primary cultured ANSCs. All data are presented as the mean ± SEM of four independent experiments. *$P < 0.05$; **$P < 0.01$; ***$P < 0.001$ vs. the indicated group.

model with β-arrestin2 knockout mice. Interestingly, β-arrestin2 deletion abolished the fluoxetine-mediated improvement of depression-like behaviors and monoamine neurotransmitter levels, although a lack of β-arrestin2 did not aggravate the CMS-induced changes in behaviors and neurotransmitters in the fluoxetine untreated group. These findings reveal that β-arrestin2 deficiency is not enough to exacerbate the phenotype of depressed mice but can weaken the antidepressant effect of fluoxetine, confirming the important role of β-arrestin2 in fluoxetine therapy.

The integration of newborn neurons into the circuitry of hippocampal neurogenesis exerts an important role in regulating memory, learning, and emotion [37, 38]. Currently, many studies have revealed that blocking adult hippocampal neurogenesis results in cognitive decline and anxiety [39]. Although fewer neural precursor cells may not be sufficient to directly show a marked difference in the detection of depression-like behaviors in mice, impairment of adult hippocampal neurogenesis has been proposed to be a crucial biological and cellular pathogenesis of depression. Furthermore, enhancement of neurogenesis can provide an important neurobiological basis for the improvement of neuronal function and the therapy of depression [40]. We thus focused on the effect of β-arrestin2 on neurogenesis in depressed mice in the present study. β-arrestin2$^{-/-}$ mice showed shortened dendritic length and reduced dendritic spine density, as well as decreased neural precursor cells under basal conditions. This finding indicates that β-arrestin2 deficiency increases the vulnerability of neurons and the susceptibility of mice to depression. Moreover, β-arrestin2 knockout decreased the number of proliferating cells in the hippocampal DG and suppressed the proliferative capability of ANSCs in vitro. Furthermore, β-arrestin2 knockout aggravated the impairment of cell proliferation induced by corticosterone and further blocked the fluoxetine-mediated promotion of mouse SGZ neurogenesis. Our findings indicate that the presence of β-arrestin2 is necessary to maintain stem cell proliferation and that the absence of β-arrestin2 may impair crucial signal transduction in regulating hippocampal neurogenesis. Moreover, the enhancement of neurogenesis by fluoxetine partially depends on β-arrestin2 expression. Similarly, Tao et al. [41] reported that β-arrestin1 knockout mice showed reduced neural precursor proliferation in the SGZ, which could be rescued by selective viral expression of β-arrestin1. Given that there was no change in β-arrestin1 expression in the CMS-induced depressive mice, we did not investigate the effect of β-arrestin1 on hippocampal neurogenesis in the present study. Even so, these findings at least suggest that both β-arrestins participate in the regulation of neural regeneration.

For the downstream β-arrestin2-mediated nonclassic signaling pathway, the PI3K/Akt pathway is the most recognized pathway to be activated by the formation of the β-arrestin-kinase complex, which is also involved in regulating cell proliferation and survival [42–44]. We found that the phosphorylation of PI3K and Akt was significantly lower in the β-arrestin2-deficient ANSCs than in the WT cells. β-arrestin2 knockout abolished the fluoxetine-mediated

activation of the PI3K/Akt pathway, which in turn eliminated the increase in cell proliferation. This effect is in line with findings showing that the PI3K inhibitor LY294002 blocked the enhancement of fluoxetine on ANSC proliferation, indicating that fluoxetine improves adult hippocampal neurogenesis via the β-arrestin2-PI3K/Akt pathway. Furthermore, the recruitment and activation of β-arrestin2 depend on GPCR expressed in the cell membrane. Different subtypes of the 5-HT receptor in ANSCs were thus identified in the present study, and we found that 5-HT_{2B}R expression was the highest among the subtypes. Previous studies have shown that fluoxetine can bind to 5-HT_{2B}R and subsequently activate this receptor in serotonergic neurons and astrocytes. However, the link between fluoxetine and 5-HT_{2B}R on ANSCs remains unknown. Our study further showed that the 5-HT_{2B}R inhibitor RS-127445 could block the activation of the PI3K/Akt pathway and subsequent improvement of ANSC proliferation induced by fluoxetine. These findings demonstrate that the 5-HT_{2B}R-β-arrestin2 axis is essential to maintain the fluoxetine-mediated modulation of hippocampal neurogenesis in depressed mice (Fig. S4).

In conclusion, this work indicates that β-arrestin2 deficiency inhibits the proliferation and survival of ANSCs and aggravates corticosterone-induced neural precursor cell injury. Importantly, the lack of β-arrestin2 abolished the fluoxetine-mediated enhancement of hippocampal neurogenesis in a depression model. This study reveals the potential role of β-arrestin2 in the pathogenesis of depression and the antidepressant effect of fluoxetine. Our study provides insight into a novel approach to treat depression depending on the 5-HT_{2B}R-β-arrestin2 axis and provides a promising molecular target for the development of new antidepressant drugs.

ACKNOWLEDGEMENTS

We would like to thank Prof. Gang Pei in Tongji University for providing β-arrestin2 knockout mice. The work reported herein was supported by the grants from the National Natural Science Foundation of China (No. 81922066, No. 81773706, No. 81991523, and No. 81630099) and the Drug Innovation Major Project (No. 2018ZX09711001-003-007).

AUTHOR CONTRIBUTIONS

ML and GH developed the concept of this study; ML and GH designed this study. CXL, YZ, HZ, CWL, ZH, CW, JHD acquired and analyzed data. CXL, YZ, and HZ drafted the figures. ML and CXL drafted the paper.

ADDITIONAL INFORMATION

The online version of this article (https://doi.org/10.1038/s41401-020-00576-2) contains supplementary material, which is available to authorized users.

Competing interests: The authors declare no competing interests.

REFERENCES

1. Abe-Higuchi N, Uchida S, Yamagata H, Higuchi F, Hobara T, Hara K, et al. Hippocampal sirtuin 1 signaling mediates depression-like behavior. Biol Psychiatry. 2016;80:815–26.
2. Moussavi S, Chatterji S, Verdes E, Tandon A, Patel V, Ustun B. Depression, chronic diseases, and decrements in health: results from the World Health Surveys. Lancet. 2007;370:851–8.
3. Bombardier CH, Fann JR, Temkin NR, Esselman PC, Barber J, Dikmen SS. Rates of major depressive disorder and clinical outcomes following traumatic brain injury. JAMA. 2010;303:1938–45.
4. Vancampfort D, Correll CU, Galling B, Probst M, De Hert M, Ward PB, et al. Diabetes mellitus in people with schizophrenia, bipolar disorder and major depressive disorder: a systematic review and large scale meta-analysis. World Psychiatry. 2016;15:166–74.
5. Herbert J, Lucassen PJ. Depression as a risk factor for Alzheimer's disease: genes, steroids, cytokines and neurogenesis - What do we need to know? Front Neuroendocrinol. 2016;41:153–71.
6. Rajkowska G, Stockmeier CA. Astrocyte pathology in major depressive disorder: insights from human postmortem brain tissue. Curr Drug Targets. 2013;14:1225–36.
7. Sanacora G, Banasr M. From pathophysiology to novel antidepressant drugs: glial contributions to the pathology and treatment of mood disorders. Biol Psychiatry. 2013;73:1172–9.
8. David DJ, Samuels BA, Rainer Q, Wang JW, Marsteller D, Mendez I, et al. Neurogenesis-dependent and -independent effects of fluoxetine in an animal model of anxiety/depression. Neuron. 2009;62:479–93.
9. Popova D, Castren E, Taira T. Chronic fluoxetine administration enhances synaptic plasticity and increases functional dynamics in hippocampal CA3-CA1 synapses. Neuropharmacology. 2017;126:250–6.
10. Gemmel M, Harmeyer D, Bogi E, Fillet M, Hill LA, Hammond GL, et al. Perinatal fluoxetine increases hippocampal neurogenesis and reverses the lasting effects of pre-gestational stress on serum corticosterone, but not on maternal behavior, in the rat dam. Behav Brain Res. 2018;339:222–31.
11. Khodanovich M, Kisel A, Kudabaeva M, Chernysheva G, Smolyakova V, Krutenkova E, et al. Effects of fluoxetine on hippocampal neurogenesis and neuroprotection in the model of global cerebral ischemia in rats. Int J Mol Sci. 2018;19:162.
12. Peng L, Gu L, Li B, Hertz L. Fluoxetine and all other SSRIs are 5-HT_{2B} agonists—importance for their therapeutic effects. Curr Neuropharmacol. 2014;12:365–79.
13. Diaz SL, Narboux-Neme N, Boutourlinsky K, Doly S, Maroteaux L. Mice lacking the serotonin 5-HT_{2B} receptor as an animal model of resistance to selective serotonin reuptake inhibitors antidepressants. Eur Neuropsychopharmacol. 2016;26:265–79.
14. Lefkowitz RJ. A brief history of G-protein coupled receptors (Nobel Lecture). Angew Chem Int Ed Engl. 2013;52:6366–78.
15. Wang W, Qiao Y, Li Z. New insights into modes of GPCR activation. Trends Pharmacol Sci. 2018;39:367–86.
16. Salazar N, Munoz D, Kallifatidis G, Singh RK, Jorda M, Lokeshwar BL. The chemokine receptor CXCR7 interacts with EGFR to promote breast cancer cell proliferation. Mol Cancer. 2014;13:198.
17. Bonnans C, Flaceliere M, Grillet F, Dantec C, Desvignes JP, Pannequin J, et al. Essential requirement for beta-arrestin2 in mouse intestinal tumors with elevated Wnt signaling. Proc Natl Acad Sci USA. 2012;109:3047–52.
18. Ravier MA, Leduc M, Richard J, Linck N, Varrault A, Pirot N, et al. beta-Arrestin2 plays a key role in the modulation of the pancreatic beta cell mass in mice. Diabetologia. 2014;57:532–41.
19. Willner P. The chronic mild stress (CMS) model of depression: History, evaluation and usage. Neurobiol Stress. 2017;6:78–93.
20. Jia M, Li C, Zheng Y, Ding X, Chen M, Ding J, et al. Leonurine exerts antidepressant-like effects in the chronic mild stress-induced depression model in mice by inhibiting neuroinflammation. Int J Neuropsychopharmacol. 2017;20:886–95.
21. Du RH, Wu FF, Lu M, Shu XD, Ding JH, Wu G, et al. Uncoupling protein 2 modulation of the NLRP3 inflammasome in astrocytes and its implications in depression. Redox Biol. 2016;9:178–87.
22. Commons KG, Cholanians AB, Babb JA, Ehlinger DG. The rodent forced swim test measures stress-coping strategy, not depression-like behavior. ACS Chem Neurosci. 2017;8:955–60.
23. Lukas M, Toth I, Reber SO, Slattery DA, Veenema AH, Neumann ID. The neuropeptide oxytocin facilitates pro-social behavior and prevents social avoidance in rats and mice. Neuropsychopharmacology. 2011;36:2159–68.
24. Brachman RA, McGowan JC, Perusini JN, Lim SC, Pham TH, Faye C, et al. Ketamine as a prophylactic against stress-induced depressive-like behavior. Biol Psychiatry. 2016;79:776–86.
25. Ramaker MJ, Dulawa SC. Identifying fast-onset antidepressants using rodent models. Mol Psychiatry. 2017;22:656–65.
26. Lu M, Yang JZ, Geng F, Ding JH, Hu G. Iptakalim confers an antidepressant effect in a chronic mild stress model of depression through regulating neuroinflammation and neurogenesis. Int J Neuropsychopharmacol. 2014;17:1501–10.
27. Kong H, Zeng XN, Fan Y, Yuan ST, Ge S, Xie WP, et al. Aquaporin-4 knockout exacerbates corticosterone-induced depression by inhibiting astrocyte function and hippocampal neurogenesis. CNS Neurosci Ther. 2014;20:391–402.
28. Fan Z, Lu M, Qiao C, Zhou Y, Ding JH, Hu G. MicroRNA-7 enhances subventricular zone neurogenesis by inhibiting NLRP3/Caspase-1 axis in adult neural stem cells. Mol Neurobiol. 2016;53:7057–69.
29. Chetty S, Friedman AR, Taravosh-Lahn K, Kirby ED, Mirescu C, Guo F, et al. Stress and glucocorticoids promote oligodendrogenesis in the adult hippocampus. Mol Psychiatry. 2014;19:1275–83.
30. Yaman OM, Erman H, Guner I, Tok OE, Pala M, Esrefoglu M, et al. Remote myocardial injury: the protective role of fluoxetine. Can J Physiol Pharmacol. 2018;96:319–27.
31. Di Rosso ME, Sterle HA, Cremaschi GA, Genaro AM. Beneficial effect of fluoxetine and sertraline on chronic stress-induced tumor growth and cell dissemination in a mouse model of lymphoma: crucial role of antitumor immunity. Front Immunol. 2018;9:1341. https://doi.org/10.3389/fimmu.2018.01341.

32. Ghosh S, Choudhury S, Mukherjee S, Gupta P, Chowdhury O, Baral R, et al. Fluoxetine triggers selective apoptosis in inflammation-induced proliferating (Ki-67(high)) thymocytes. Immunol Cell Biol. 2019;97:470–84.
33. Hu HM, Li B, Wang XD, Guo YS, Hui H, Zhang HP, et al. Fluoxetine is neuroprotective in early brain injury via its anti-inflammatory and anti-apoptotic effects in a rat experimental subarachnoid hemorrhage model. Neurosci Bull. 2018;34:951–62.
34. Casarini L, Reiter E, Simoni M. beta-arrestins regulate gonadotropin receptor-mediated cell proliferation and apoptosis by controlling different FSHR or LHCGR intracellular signaling in the hGL5 cell line. Mol Cell Endocrinol. 2016;437:11–21.
35. Kallifatidis G, Munoz D, Singh RK, Salazar N, Hoy JJ, Lokeshwar BL. Beta-arrestin-2 counters CXCR7-mediated EGFR transactivation and proliferation. Mol Cancer Res. 2016;14:493–503.
36. Kong Z, Deng T, Zhang M, Zhao Z, Liu Y, Luo L, et al. Beta-arrestin1-mediated inhibition of FOXO3a contributes to prostate cancer cell growth in vitro and in vivo. Cancer Sci. 2018;109:1834–42.
37. Lazarov O, Hollands C. Hippocampal neurogenesis: learning to remember. Prog Neurobiol. 2016;138-140:1–18.
38. Toda T, Gage FH. Review: adult neurogenesis contributes to hippocampal plasticity. Cell Tissue Res. 2018;373:693–709.
39. Jesulola E, Micalos P, Baguley IJ. Understanding the pathophysiology of depression: from monoamines to the neurogenesis hypothesis model - are we there yet? Behav Brain Res. 2018;341:79–90.
40. Micheli L, Ceccarelli M, D'Andrea G, Tirone F. Depression and adult neurogenesis: positive effects of the antidepressant fluoxetine and of physical exercise. Brain Res Bull. 2018;143:181–93.
41. Tao Y, Ma L, Liao Z, Le Q, Yu J, Liu X, et al. Astroglial beta-arrestin1-mediated nuclear signaling regulates the expansion of neural precursor cells in adult hippocampus. Sci Rep. 2015;5:15506.
42. Wang Y, Jin L, Song Y, Zhang M, Shan D, Liu Y, et al. Beta-arrestin 2 mediates cardiac ischemia-reperfusion injury via inhibiting GPCR-independent cell survival signalling. Cardiovasc Res. 2017;113:1615–26.
43. Eichel K, Jullie D, von Zastrow M. Beta-arrestin drives MAP kinase signalling from clathrin-coated structures after GPCR dissociation. Nat Cell Biol. 2016;18:303–10.
44. Manago F, Espinoza S, Salahpour A, Sotnikova TD, Caron MG, Premont RT, et al. The role of GRK6 in animal models of Parkinson's disease and *L*-DOPA treatment. Sci Rep. 2012;2:301.